

UC San Diego

UC San Diego Previously Published Works

Title

Ion mobility derived collision cross sections to support metabolomics applications.

Permalink

<https://escholarship.org/uc/item/6nk9s2p7>

Journal

Analytical chemistry, 86(8)

ISSN

0003-2700

Authors

Paglia, Giuseppe
Williams, Jonathan P
Menikarachchi, Lochana
[et al.](#)

Publication Date

2014-04-01

DOI

10.1021/ac500405x

Peer reviewed

Ion Mobility Derived Collision Cross Sections to Support Metabolomics Applications

Giuseppe Paglia,^{*,†} Jonathan P. Williams,[‡] Lochana Menikarachchi,[§] J. Will Thompson,^{||} Richard Tyldesley-Worster,[‡] Skarphédinn Halldórsson,[†] Ottar Rolfsson,[†] Arthur Moseley,^{||} David Grant,[§] James Langridge,[‡] Bernhard O. Palsson,^{†,⊥} and Giuseppe Astarita^{*,#,§}

[†]Center for Systems Biology, University of Iceland, IS 101, Reykjavik, Iceland

[‡]Waters Corporation, Manchester M23 9LZ, U.K.

[§]Department of Pharmaceutical Sciences, University of Connecticut, Storrs, Connecticut 06269, United States

^{||}Duke Proteomics Core Facility, Durham, North Carolina 27710, United States

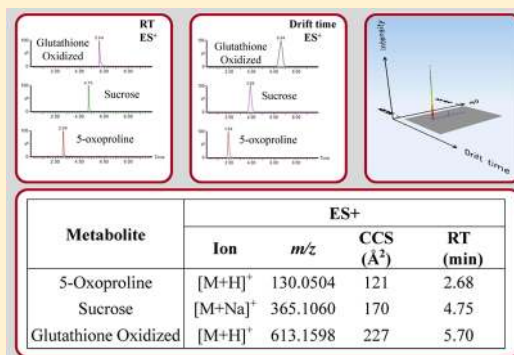
[⊥]Systems Biology Research Group, University of California San Diego, La Jolla, California 92093, United States

[#]Waters Corporation, Milford, Massachusetts 01757, United States

[§]Georgetown University, Washington, District of Columbia 20057, United States

S Supporting Information

ABSTRACT: Metabolomics is a rapidly evolving analytical approach in life and health sciences. The structural elucidation of the metabolites of interest remains a major analytical challenge in the metabolomics workflow. Here, we investigate the use of ion mobility as a tool to aid metabolite identification. Ion mobility allows for the measurement of the rotationally averaged collision cross-section (CCS), which gives information about the ionic shape of a molecule in the gas phase. We measured the CCSs of 125 common metabolites using traveling-wave ion mobility-mass spectrometry (TW-IM-MS). CCS measurements were highly reproducible on instruments located in three independent laboratories (RSD < 5% for 99%). We also determined the reproducibility of CCS measurements in various biological matrixes including urine, plasma, platelets, and red blood cells using ultra performance liquid chromatography (UPLC) coupled with TW-IM-MS. The mean RSD was < 2% for 97% of the CCS values, compared to 80% of retention times. Finally, as proof of concept, we used UPLC–TW-IM-MS to compare the cellular metabolome of epithelial and mesenchymal cells, an in vitro model used to study cancer development. Experimentally determined and computationally derived CCS values were used as orthogonal analytical parameters in combination with retention time and accurate mass information to confirm the identity of key metabolites potentially involved in cancer. Thus, our results indicate that adding CCS data to searchable databases and to routine metabolomics workflows will increase the identification confidence compared to traditional analytical approaches.



Metabolomics, a powerful analytical strategy in translational medicine and biomarker discovery, relies on advanced technology to profile metabolites in cells, tissues, and biofluids.^{1–3} The confident identification of these metabolites on a high-throughput scale, however, remains a major analytical challenge because of their chemical and structural diversity. Thus, implementing workflows that involve orthogonal analytical tools might facilitate metabolite identification.⁴

Mass spectrometry (MS) is a widely used technique for analyzing small molecules.⁵ Because of the complexity of the metabolome, MS-based metabolomics analyses are usually performed in conjunction with liquid chromatography (LC).⁵ Analyzing hydrophilic compounds by means of traditional reversed-phase LC–MS is not ideal as these metabolites are poorly retained and usually elute in the void volume.^{6,7} On the

other hand, it has been demonstrated that hydrophilic interaction liquid chromatography–MS (HILIC–MS) improves resolution, identification, and quantification for these types of compounds.^{7–10} Intersample variability caused by using different matrixes and sample loading, however, can lead to shifts in retention times, which complicates the use of retention time for identification purposes.

The coupling of UPLC with ion mobility MS (UPLC–IM–MS) is a promising analytical technique within the field of metabolomics.^{11–16} Ion mobility spectrometry is a gas-phase electrophoretic technique that separates ions according to their

Received: January 24, 2014

Accepted: March 18, 2014

Published: March 18, 2014

charge, shape, and size. Ion separation occurs in the millisecond time frame, making it compatible with time-of-flight mass spectrometry. The CCS¹⁷ for a given ion can be derived by measuring the time required for an ion to traverse a chamber filled with an inert gas. The CCS value is a unique physicochemical property of a molecule. Using CCS as an orthogonal molecular descriptor in addition to retention time and mass-to-charge ratio (m/z) offers the opportunity to further improve the identification process, making it more robust and reproducible across multiple samples and time-frames.^{13–16,18–23} Such an approach remains largely unexplored in metabolomics applications.

During this study, we incorporated ion mobility into the UPLC–MS, metabolomics workflow. We generated a CCS database of common cellular metabolites, validated across multiple laboratories, which was ultimately used to confidently identify the metabolic alterations related to the epithelial–mesenchymal transition process. Our study highlights the benefit of using ion mobility in metabolomics

■ EXPERIMENTAL SECTION

Chemicals. All materials were obtained from Sigma-Aldrich (Germany) unless stated otherwise. Acetonitrile (ACN) was purchased from Merck KGaA, (Darmstadt, Germany). Water was obtained using an 18 Ω m Milli-Q (EMD Millipore Corporation, Billerica, MA). All chemicals and solvents were of analytical grade or higher purity. Poly-DL-alanine (product number P9003) was purchased from Sigma-Aldrich (U.K.). Platelets (PLT), red blood cells (RBC), and plasma were obtained from the Blood Bank, Landspítali-University Hospital, Reykjavik, Iceland). Urine was obtained from a male volunteer. This study was approved by the National Bioethics Committee of Iceland and the Icelandic Data Protection Authority.

Sample Preparation. Standard Mixtures. Mixtures containing between 10 and 15 standard metabolites (each with a different molecular weight) were prepared in H₂O/ACN (50:50, v:v), at a concentration of 10 mg/L.

Biological Samples. A volume of 0.5 mL of PLT and RBC concentrates were used to extract intracellular metabolites using methanol (MeOH)/H₂O (7:3, v:v), as previously described.⁷ The supernatant was dried and reconstituted in 0.3 mL of H₂O/ACN (50:50, v:v). Plasma samples (0.3 mL) were processed by adding 0.9 mL of MeOH. After centrifugation (10 min, 4 °C, 10 000g), the supernatant was dried and reconstituted in 0.15 mL of H₂O/ACN (50:50, v:v). Urine samples (0.2 mL) were processed adding 0.6 mL of MeOH. After centrifugation (10 min, 4 °C, 10 000g), the supernatant was dried and reconstituted in 0.5 mL of H₂O/ACN (50:50, v:v).

Cell Culture. D492 breast epithelial cells and D492M, epithelially derived mesenchymal cells were cultured as previously described.²⁴ Briefly, cells were cultured to confluency in H14 medium at 37 °C and 5% CO₂. After 3 days in culture, the cells were trypsinized, collected by centrifugation, counted, and washed three times with PBS. Intracellular metabolites were extracted using MeOH/H₂O (7:3 v:v) as previously described.⁷

MS Analysis. Three traveling-wave ion mobility mass spectrometers (TW-IM-MS)²⁵ (Synapt G2 HDMS, Waters Corporation, Manchester, U.K.) located in independent laboratories were used to derive CCS information for a variety of small low molecular weight, polar metabolites (Table S1 in the Supporting Information).

The first Synapt HDMS system was located in Durham, NC. In positive electrospray mode, the capillary and cone voltage were 2.6 kV and 35 V, respectively. The source and desolvation temperatures were 100 and 150 °C, respectively, and the desolvation gas flow was 600 L/h. Nitrogen, the IMS gas, flowed at a rate of 90 mL/min (3.2 mbar), with a wave velocity of 600 m/s and wave height of 40 V. In negative electrospray mode, the capillary and cone voltage were 2.3 kV and 25 V, respectively. The source and desolvation temperature were 100 and 150 °C, respectively, and the desolvation gas flow was 600 L/h. Nitrogen, the IMS gas, flowed at a rate of 90 mL/min (3.2 mbar), with a wave velocity of 650 m/s and wave height of 40 V. The EDC delay coefficient was specified as 1.36 V in positive mode and as 1.41 in negative mode. In both positive and negative mode, direct injection at a flow rate of 0.75 μ L/min was used.

The second Synapt HDMS system was located in Manchester, U.K. In positive electrospray mode, the capillary and cone voltage were 2.5 kV and 30 V, respectively. The source and desolvation temperature were 100 and 250 °C, respectively, and the desolvation gas flow was 600 L/h. Nitrogen, the IMS gas, flowed at a rate of 90 mL/min (3.2 mbar), with a wave velocity of 750 m/s and wave height of 40 V. In negative electrospray mode, the capillary and cone voltage were 2 kV and 40 V, respectively. The source and desolvation temperature were 100 and 250 °C, respectively, and the desolvation gas flow was 600 L/h. Nitrogen, the IMS gas, flowed at a rate of 90 mL/min (3.2 mbar), with a wave velocity of 800 m/s and wave height of 40 V. The EDC delay coefficient was specified as 1.58 V. Direct injection at a flow rate of 5 μ L/min was used in both positive and negative mode.

The third Synapt HDMS system was located in Reykjavik, Iceland. In positive electrospray mode, the capillary and cone voltage were 1.5 kV and 30 V, respectively. The source and desolvation temperature were 120 and 500 °C, respectively, and the desolvation gas flow was 800 L/h. Nitrogen, the IMS gas, flowed at a rate of 90 mL/min (3.2 mbar), with a wave velocity of 600 m/s and wave height of 32 V. In negative electrospray mode, the capillary and cone voltage were 1.5 kV and 30 V, respectively. The source and desolvation temperature were 120 and 500 °C, respectively, and the desolvation gas flow was 800 L/h. Nitrogen, the IMS gas, flowed at a rate of 90 mL/min (3.2 mbar), with a wave velocity of 600 m/s and wave height of 32 V. The EDC delay coefficient was specified as 1.58 V. Argon served as collision gas in both positive and negative mode. During HDMS^E experiments, the collision energy in the trap cell was 4 eV (Function 1), and in the transfer cell, it ranged from 20 to 30 eV (Function 2). In both positive and negative mode, direct injection, at a flow rate of 0.75 μ L/min, or UPLC was used.

Liquid Chromatographic Analysis. Chromatographic separation was achieved using an ACQUITY UPLC system (UPLC ACQUITY, Waters Corporation, Milford, MA) and hydrophilic-interaction liquid chromatography (HILIC) using a 1.7- μ m (2.1 mm \times 150 mm) ACQUITY amide column (Waters Corporation). Samples and standard mixtures were analyzed three times in UPLC–HILIC–HDMS^E, once in positive ionization mode and twice in negative ionization mode using acidic and basic chromatographic conditions, respectively. In positive mode and in negative acidic conditions alike, mobile phase A was 100% ACN and mobile phase B was 100% H₂O, with both containing 0.1% formic acid. The following elution gradient was used: 0 min, 99% A; 6 min, 40%

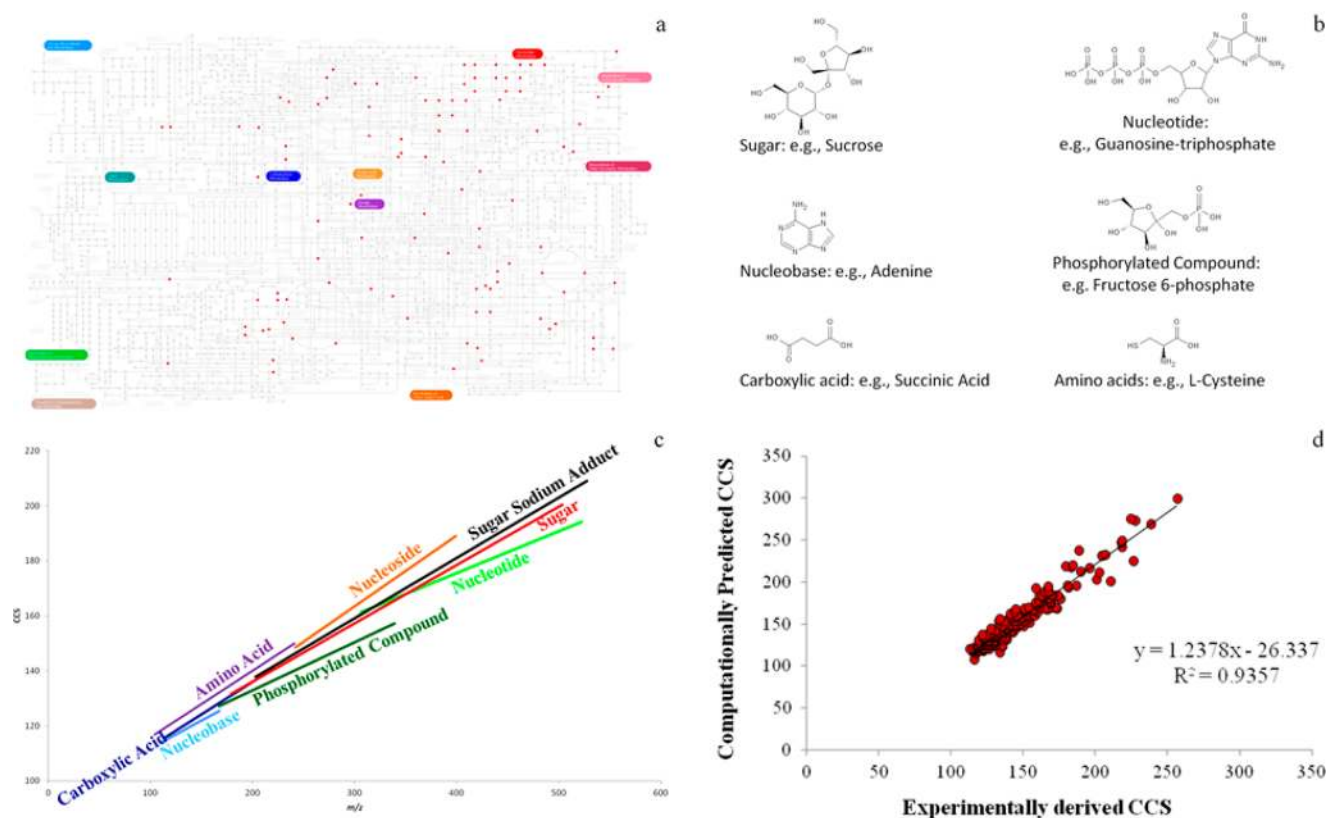


Figure 1. CCS measurements for 125 common metabolites: (a) visual representation of the metabolites analyzed in this study (red dots) according to their metabolic position in a KEGG metabolic map. (b) Classes of cellular metabolites included in this study. (c) Correlation between CCS and mass values. Both CCS value in negative and positive modes were used, and sodium adducts were excluded except for sugars: amino acids and derivatives ($n = 55$, $R = 0.91$); carboxylic acids ($n = 9$, $R = 0.90$); nucleobases ($n = 16$, $R = 0.88$); phosphorylated compounds ($n = 15$, $R = 0.84$); sugar ($n = 13$, $R = 0.99$); sugar sodium adducts ($n = 12$, $R = 0.99$); nucleosides ($n = 19$, $R = 0.94$); nucleotides ($n = 23$, $R = 0.81$). (d) Correlation between experimentally derived and computationally predicted CCS values.

A; 8 min, 99% A; 10 min, 99% A. In negative-mode basic conditions, mobile phase A contained ACN/sodium bicarbonate, 10 mM (95:5) and mobile phase B contained ACN/sodium bicarbonate, 10 mM (5:95). The following elution gradient was used: 0 min, 99% A; 5 min, 42% A; 6 min, 70% A; 7 min, 99%; 10 min, 99% A. In all conditions, the flow rate was 0.4 mL/min, the column temperature 45 °C, and the injection volume 3.5 μ L.

CCS Measurements for Metabolites. CCS values obtained in nitrogen were experimentally determined using previously published CCS values for singly charged polyalanine oligomers as the TW mobility calibrant^{26,27} (Table S2, Supporting Information). Experimental procedures for measuring CCS are outlined in Figure S1 (see the Supporting Information for more details). Poly-DL-alanine was used as the calibrant species in both electrospray positive (ES^+) and ES^- and was prepared in H_2O/ACN (50:50, v:v) at a concentration of 10 mg/L. Calibration was performed using oligomers from $n = 3$ to $n = 11$, covering a mass range from 231 to 799 Da and a CCS range from 151 \AA^2 to 306 \AA^2 in ES^+ and from 150 \AA^2 to 308 \AA^2 in ES^- (Table S2, Supporting Information).²⁶ CCSs were derived using a procedure previously reported.²⁶ The ion mobility resolution was ~ 40 (fwhm). The ion mobility peak or arrival time distribution (ATD) may represent a combination of structurally similar isomers that remain unresolved. The CCS values reported were determined at the apex of the ion mobility peak or ATD. The use of different ionization sources (causing different interferences that are not resolved) and/or different

mobility calibrants could lead to slight variations in the reported CCS.²⁸

Prediction of CCS via Computational Methods.

Theoretical collisional cross sections were calculated as follows. First, two-dimensional (2D) structures for the compounds were downloaded from NCBI's PubChem database²⁹ in SD file format. Following this, ChemAxon's (ChemAxon, 5.4.1.1.) pK_a module was used to calculate the most acidic or most basic atom in each 2D structure. Protonated and sodiated forms were generated by connecting a hydrogen or a sodium atom to the most basic atom in the 2D structure. The formal charge of the most basic atom was then set to +1. Similarly, a hydrogen attached to the most acidic atom was disconnected to generate deprotonated structures. Then, ChemAxon's conformer plugin was used to generate molecular mechanics (using MMFF94 force field) based lowest energy conformers. Each molecular mechanics based minimum energy conformer was reoptimized with the density functional theory B3LYP/6-31g*. Density functional calculations were done with Gaussian09.³⁰ All structure manipulations (generation of ionized forms and molecular mechanics based conformers) and input file preparations (for Gaussian09 and Mobcal) were done using MolFind's tools panel.³¹ Finally, a modified version of Mobcal^{32–34} optimized according to the room temperature N_2 -based trajectory method (TM) was used for calculating average collision cross-sectional areas.

Data Processing and Analysis. Progenesis QI v1.0 (Nonlinear Dynamics, Newcastle, U.K.) was used for visual-

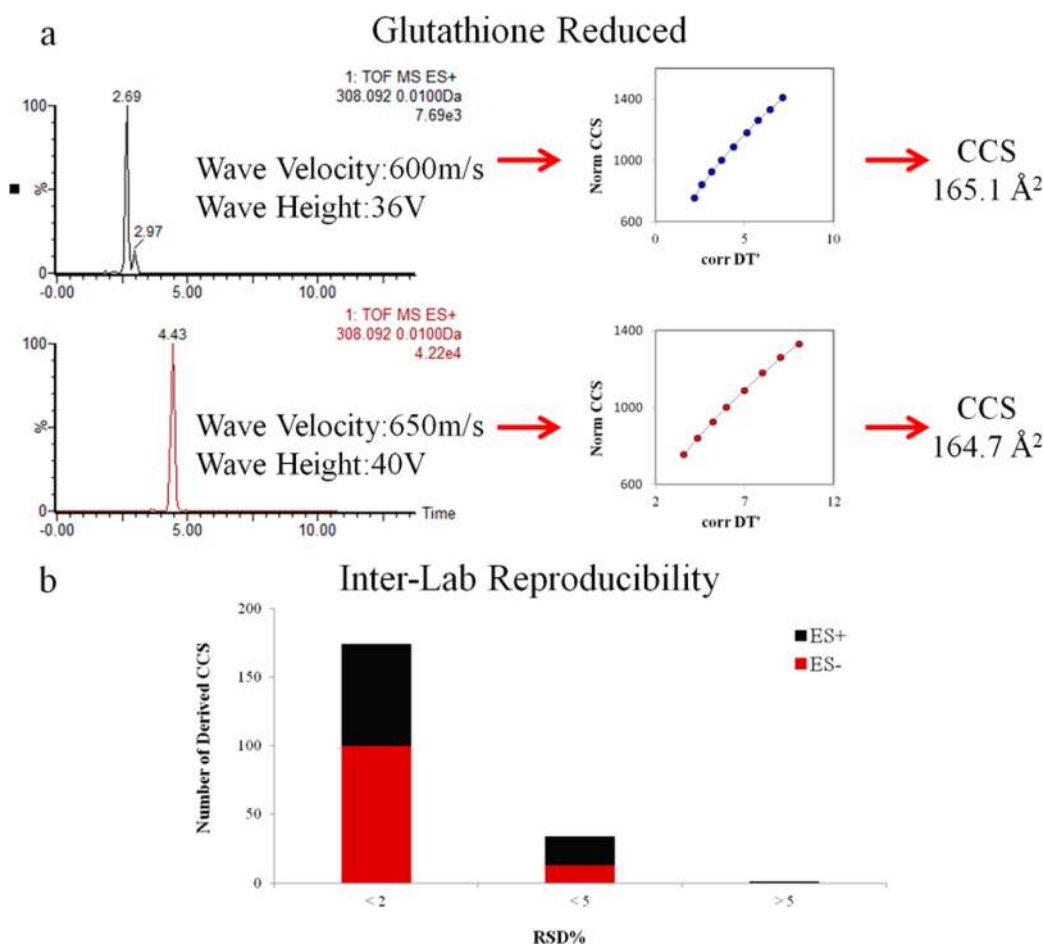


Figure 2. Reproducibility of CCS measurements across different instruments: (a) different drift time values for reduced glutathione were obtained using different TW-IM parameter settings. The use of polyaniline as calibrators corrected the final CCSs measurements. (b) Relative standard deviation (RSD%) for CCS measurements across three independent laboratories.

ization, processing, and interpretation of multidimensional IM-MS data. Each UPLC-IM-MS run was imported as an ion intensity map, including m/z and retention time. These ion maps were then aligned in the retention time direction. From the aligned runs, Progenesis Q1 produces an aggregate run that was representative of the compounds in all samples and used this aggregate run for peak picking. The peak picking from this aggregate was then propagated to all runs, so that the same ions are detected in every run. Isotope and adduct deconvolution was applied to reduce the number of features detected. Data were normalized using total ion intensity. The software was coded to directly convert drift time data into CCS values using the polyaniline calibration curve. Statistically significant alterations were identified using multivariate statistics, including principal components analysis (PCA) and orthogonal partial least square-discriminant analysis (OPLS-DA) and further confirmed using analysis of variance (ANOVA). Metabolites were identified by searching in the Human Metabolome Database (HMDB),³⁵ METLIN,^{36,37} and in-house databases with $\Delta\text{ppm} < 10$, retention time range < 0.3 s, and $\Delta\text{CCS} < 5$ Å² as tolerance parameters. Fragment ion mass spectra were analyzed in both MS^E and HDMS^E mode.

RESULTS AND DISCUSSION

Investigating the use of ion mobility to support metabolomic applications, we conducted a multilaboratory study to obtain

the CCS values of 125 standard metabolites, using both experimentally derived and computationally calculated approaches. This data was used to create a unique database, which contained not only retention time and m/z information, but also CCS values for each structure. In order to validate the database and its unique capabilities, we conducted metabolomics analyses of biological samples using the additional CCS information to aid in the identification of metabolites.

Experimentally- and Computationally Derived CCSs of Common Metabolites. Experimental procedures for measuring CCSs are based on calibration with compounds having known CCS values as reported in the Experimental Section (Figure S1, Supporting Information). In order to represent the chemical complexity of the cellular metabolome, we selected as unknowns 125 metabolites representing key metabolic pathways. These metabolites included sugars, phosphorylated compounds, purines and pyrimidines, nucleotides, nucleosides, acylcarnitines, carboxylic acids, hydrophilic vitamins and amino acids (Figure 1 and Table S3 in the Supporting Information). We measured drift times in nitrogen for these metabolites using TW-IM-MS instruments located in three independent laboratories (Table S4, Supporting Information). We then derived CCS values using polyaniline oligomers as mobility calibrants in both positive and negative ES mode of operation. The polyaniline standards allowed us to correct for variation in drift times between instruments located in different laboratories and having different ion mobility

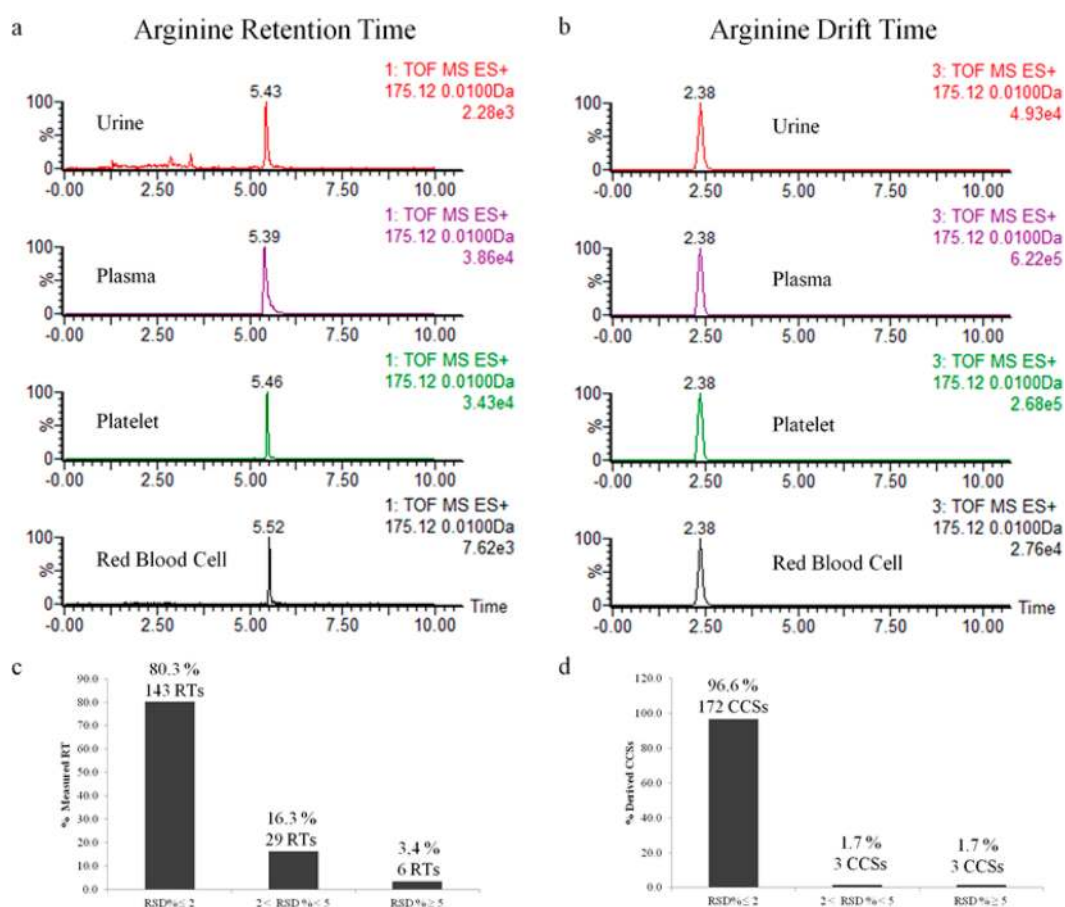


Figure 3. Matrix effect on retention times compared to CCSs: (a) extracted-ion chromatograms and (b) extracted-ion mobility chromatograms of arginine analyzed in four different biological matrixes (plasma, red blood cells, platelets, and urine). (c) Retention times reproducibility and (d) CCSs reproducibility in the various biological matrixes.

parameter settings (Figure 2a). We derived 209 CCS values (96 in positive and 113 in negative ion mode) with an interlaboratory RSD% lower than 5% for 99% of the measurements (Figure 2b). These results support the proposition that a CCS value derived from calibration is an absolute measurement, representing a physicochemical property that is consistent across a range of experimental and instrumental conditions. Experimentally derived CCS values highlighted trend lines related to different chemical classes (Figure 1c). Furthermore, experimentally derived CCS values correlated closely with theoretical CCS calculated using Mobcal (Figure 1d and Table S4, Supporting Information).

Generation of a Database Containing Retention Time, CCS, and m/z Values. To allow a more comprehensive LC separation of the different classes of compounds used in this study, we coupled UPLC with TW-IM-MS. Notably, the analysis of polar metabolites using traditional reversed-phase LC-MS presents some challenges because they are poorly retained and usually eluted in the void volume.^{6–10} Two different HILIC methods (i.e., acidic and basic) were used (for details see the Experimental Section). Basic conditions were chosen to separate phosphorylated compounds, such as nucleotides and sugar phosphates, which under acidic conditions were strongly retained, resulting in poor chromatographic peak shape.^{7,8} Using HILIC conditions, our set of polar metabolites eluted in order of increasing polarity (Table S3, Supporting Information). For each of the 125 compounds included in this study, we annotated values for accurate mass,

CCS, and retention time, creating a database that was then used to analyze biological samples.

Application of Ion Mobility-Derived Information to the Analysis of Biological Samples. To evaluate the applicability of this approach to metabolomic applications, we analyzed plasma, urine, red blood cells (RBCs), and platelets (PLTs) using UPLC-TW-IM-MS. In these experiments, we calculated the Δ CCS (the difference between the database CCS and the experimental CCS) and used this as a contribution to the identification score in addition to retention time and accurate mass. This enabled us to search for metabolites whose identifications have a CCS error less than a given threshold. Thus, we were able to filter and score identifications when querying our database with CCS information. Using CCS, retention time, and accurate mass as orthogonal coordinates, a total of 94 different metabolites were confirmed to be present in the various biological matrixes (48 in plasma, 46 in urine, 74 in RBCs, and 71 in PLTs).

The retention time of a given metabolite can change from one run to the next due to experimental drift (e.g., room/column temperature and degradation of the column). Moreover, different sample matrixes can influence the reproducibility of retention times, largely due to different salt and lipid contents. Figure 3a shows the extracted-ion chromatogram of arginine in different matrixes, highlighting the effect of the matrix on retention time. In Figure 3b, we present the extracted-ion chromatogram resulting from the ion mobility separation showing the absence of the matrix effect on drift

Metabolite	HMDB ID	Formula	m/z	RT (min)	CCS (\AA^2)	Mass Error (ppm)	Δ RT (mins)	Δ CCS (%)	Isotope Similarity
Guanosine	HMDB00133	C ₁₀ H ₁₃ N ₅ O ₅	282.0840	3.97	157.5	0.7	-0.04	0.1	92.3
Inosine	HMDB00195	C ₁₀ H ₁₂ N ₄ O ₅	267.0728	3.56	153.1	-0.5	-0.08	0.4	95.0
Inosine Fragment		C ₅ H ₄ N ₄ O	135.0309	3.56	123.6	1.5	0.26	5.2	95.6

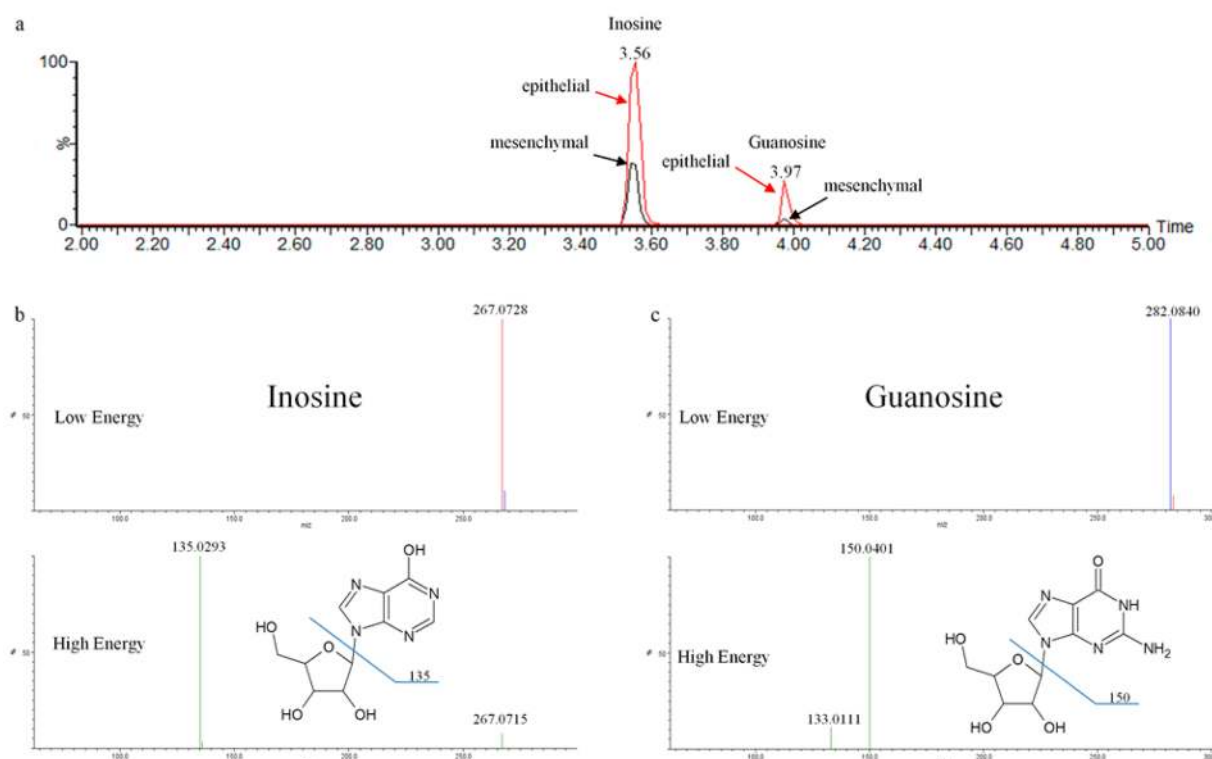


Figure 4. Experimentally determined CCS information in support of metabolite identification. Retention times, m/z , CCS, isotopic pattern, and fragmentation information were used to identify metabolites that had a statistically significant alteration during the epithelial–mesenchymal transition process: (a) overlaid, extracted-ion chromatograms of inosine and guanosine in epithelial and mesenchymal cells. (b) Low- and high-energy spectra for inosine in HDMS^E mode. (c) Low- and high-energy spectra for guanosine in HDMS^E mode. Data processing and analysis performed using Progenesis Q1 v1.0.

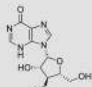

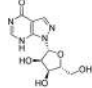
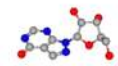
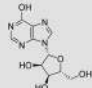

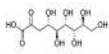
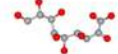
time. Our results showed a RSD% <2 for 97% of the CCS measurements, compared with 80% for the retention time values, suggesting that CCS measurements are more stable and reliable than retention time and thus may add more confidence in the identification process during metabolomics experiments (Figure 3c,d).

To confirm the identity of the metabolites, we performed the analysis using data-independent or UPLC–“MS^E” mode of acquisition, which alternates between a low and elevated collision energy regime. At low collision energy, the exact mass measurements of unfragmented precursor ions are obtained, whereas at the elevated collision energy, the product ions for all precursors are obtained.^{38,39} In biological samples, however, multiple analytes often have indistinguishable retention times. Consequently, applying elevated collision energy in MS^E mode might lead to the generation of product ions derived from multiple precursor ions at a given retention time, complicating the identification process (Figure S2, Supporting Information). To overcome this problem, we used a combination of MS^E and ion mobility, HDMS^E, which allows the drift time separation of coeluting precursor metabolites before the fragmentation process takes place. Precursor ions and fragment ions were ion mobility-aligned to filter out fragments that do not match the precursor’s drift time. Precursor separation was important

for obtaining a cleaner collision-induced dissociation spectrum that is not contaminated from a mixture of coeluting compounds. The use of ion mobility thus provided a simplified and cleaned product ion spectrum that facilitated the identification process (Figure S2, Supporting Information). HDMS^E ultimately resulted in a better performance in terms of converting feature detected in metabolites identified, increasing the ratio feature/metabolites compared to a typical LC–MS.⁴⁰ Such results are in agreement with previous studies showing that HDMS^E provides better clarity and depth of coverage for the analysis of complex samples compared to regular MS approaches.^{41–43} In an in depth analysis of the precision and accuracy of HDMS^E, it has been shown that with ion mobility activated, the number of ion detections and accurate-mass retention-time pairs increased at an average rate of 24.4 and 26.6%, respectively, while at the same time, the average number of ion interference events dropped from 20.2 to 5.4%.^{41–43}

Application of Ion Mobility-Derived Information to Metabolomics. We applied the approach described above to investigate the metabolic alterations occurring during the epithelial–mesenchymal transition process. Such a process occurs during embryonic development whereby epithelial cells acquire mesenchymal, fibroblast-like properties and display reduced intracellular adhesion and increased motility. It is also

Table 1. List of Potential Metabolite Candidates for m/z 267.0728 after a Search in the HMDB Database with a Cutoff of 5 ppm^a

HMDB hits for m/z 267.0728 (<5ppm)	HMDB ID	Δ ppm	Structure	3D Structure	Theoretical CCS	Experimental CCS	Δ^1 CCS (\AA^2)	Δ^1 CCS (%)
Arabinosyl-hypoxanthine	HMDB03040	-0.55			168.23		15.13	9.88
Allopurinol-1-ribonucleoside	HMDB00481	-0.55			160.11		7.01	4.58
Inosine	HMDB00195	-0.55			159.49	153.1	6.39	4.17
3-Deoxy-D-glycero-D-galacto-2-nonulosonic acid	HMDB00425	4.44			143.94		-9.16	-5.98

^aTheoretical CCS values were compared with the experimental CCS value for inosine to generate Δ^1 CCS in support of mass measurement to aid metabolite identification. Three-dimensional structures of energy-minimized metabolites showing the different conformations after molecular modeling.

the means by which malignant epithelial tumors metastasize.^{24,44,45} This tightly regulated process is associated with a number of cellular and molecular events, many of which are not yet characterized.

In order to shed light on the metabolic events leading to the differentiation of epithelial and mesenchymal cells, we compared the metabolome of D492 breast epithelial cells ($n = 4$) with that of D492 M epithelially derived mesenchymal cells ($n = 4$) using HILIC UPLC–TW-IM-MS. Data processing and analysis highlighted three molecular features as major contributors to the variance between epithelial and mesenchymal cells (Figure 4 and Figure S3, Supporting Information). The accurate-mass measurements of these discriminating features were searched against HMDB and METLIN and resulted in a list of potential identifications based on accurate-mass error (<5 ppm). Review of such a list was supported by the use of HDMS^E fragmentation spectra, retention time, and isotopic pattern deviation (Figure 4). Drift time data of unknown species were directly converted to CCS values by calibrating with polyalanine ions of known CCS, providing an additional coordinate for metabolite characterization (Figure 4 and Figure S3, Supporting Information). Comparing the experimental CCS values with those reported in our database, we were able to confirm the identity of inosine and guanosine as two of the features of interest (Δ CCS = 0.1% \AA^2 for inosine and Δ CCS = 0.4% \AA^2 for guanosine) (Figure 4). The third molecular feature at m/z 135.0309 was identified as a hypoxanthine-like fragment derived from in-source breakdown of inosine (Figure 4). These results indicate that CCS can be used as an orthogonal analytical parameter alongside the traditional molecular identifiers of precursor accurate mass, fragment ion accurate mass, isotope pattern, and chromatographic retention time as a confirmation of metabolite identity to increase the confidence of identification.⁴⁶

An obvious limitation of this approach is that it is impractical to prepare a completely comprehensive database containing experimental CCS's for all compounds present across metabolomes. An alternative strategy that would potentially alleviate this problem is the use of computationally predicted CCSs.³¹ In cases where mass measurements and Δ ppm are not

able to differentiate between potential candidate metabolites obtained from a database search, a comparison between the experimental and theoretical CCS values can support the identification process. As an example, the accurate m/z at 267.0728 for inosine was searched against the HMDB and METLIN database leading to four potential candidates, with Δ ppm < 5 ppm (Table 1). Three out of the four matches had identical Δ ppm values but different CCS values. In such a case, Δ^1 CCS (the difference between the theoretical CCS and the experimental CCS) was used to filter the potential candidates, increasing the confidence of identification for inosine (the compound with the lowest Δ^1 CCS, Table 1). These results indicate that computationally predicted CCS might be used as an indicator of compound structure to aid metabolite identification during searches in large metabolite database, potentially reducing the number of false positive and false negative identifications.

CONCLUSIONS

In this study, we integrated ion mobility into a typical LC–MS-based workflow for routine metabolomics applications. The use of ion mobility in combination with UPLC–MS and UPLC–MS/MS increased the system peak capacity and specificity for metabolite identification. Ion mobility was used to measure CCS values for 125 metabolites across three independent laboratories, demonstrating high intra- and interlaboratory reproducibility. The creation of a searchable database for metabolites that includes CCS as an orthogonal analytical measurement, in addition to retention time and m/z , increased the confidence of metabolite identification compared to traditional LC–MS approaches. Metabolomics applications using direct infusion or desorption ionization sources in combination with TW-IM-MS could particularly benefit from the use of CCS-containing databases to support metabolite identification.^{20,47–49} We encourage further studies to extend and populate existing metabolite databases with CCS values for metabolomics and other small molecules applications.

■ ASSOCIATED CONTENT**■ Supporting Information**

(a) Procedure for deriving CCS using a Synapt HDMS^E; (b) summary of MS settings; (c) polyalanine CCS reference values; (d) database of polar metabolites, including retention time, *m/z*, and CCS values; (e) data set containing experimental and predicted CCS values; (f) workflow of the experimental procedure utilized to measure CCS; (g) comparison of MS^E and HDMS^E acquisition modes for metabolomics analyses; and (h) multivariate statistics analysis for the identification of metabolites most responsible for differences between epithelial and mesenchymal cells. This material is available free of charge via the Internet at <http://pubs.acs.org>.

■ AUTHOR INFORMATION**Corresponding Authors**

*E-mail: beppepaglia@gmail.com.

*E-mail: giuseppe_astarita@waters.com

Notes

The authors declare no competing financial interest.

■ ACKNOWLEDGMENTS

This work was partly supported by the European Research Council, Grant Proposal No. 232816 (to B.O.P.), NIH Grant 1R01GM087714 (to D.G.), and Grant NIRG-11-203674 (to G.A.). The authors would like to thank Dr. Matthew Bush for providing CCS values in nitrogen for polyalanine in negative and positive mode, Miss Soley Valgeirsdottir for technical support, and Dr. Ólafur E. Sigurjónsson and Dr. Sveinn Gudmundsson for providing plasma, red blood cells, and the platelets sample. The authors would like to thank also Drs. Kevin Giles, Scott Geromanos, Mark Wrona, Keith Richardson, and Russell Mortishire-Smith for the useful discussions.

■ REFERENCES

- (1) Patti, G. J.; Yanes, O.; Siuzdak, G. *Nat. Rev. Mol. Cell. Biol.* **2012**, *13*, 263–269.
- (2) Heather, L. C.; Wang, X.; West, J. A.; Griffin, J. L. *J. Mol. Cell. Cardiol.* **2013**, *55*, 2–11.
- (3) Dunn, W. B.; Broadhurst, D. I.; Atherton, H. J.; Goodacre, R.; Griffin, J. L. *Chem. Soc. Rev.* **2011**, *40*, 387–426.
- (4) Dunn, W. B.; Broadhurst, D.; Begley, P.; Zelena, E.; Francis-McIntyre, S.; Anderson, N.; Brown, M.; Knowles, J. D.; Halsall, A.; Haselden, J. N.; Nicholls, A. W.; Wilson, I. D.; Kell, D. B.; Goodacre, R.; The Human Serum Metabolome (HUSERMET) Consortium. *Nat. Protoc.* **2011**, *6*, 1060–1083.
- (5) Dettmer, K.; Aronov, P. A.; Hammock, B. D. *Mass Spectrom. Rev.* **2007**, *26*, 51–78.
- (6) Ivanisevic, J.; Zhu, Z. J.; Plate, L.; Tautenhahn, R.; Chen, S.; O'Brien, P. J.; Johnson, C. H.; Marletta, M. A.; Patti, G. J.; Siuzdak, G. *Anal. Chem.* **2013**, *85*, 6876–6884.
- (7) Paglia, G.; Magnusdottir, M.; Thorlacius, S.; Sigurjonsson, O. E.; Guethmundsson, S.; Palsson, B. O.; Thiele, I. *J. Chromatogr., B: Anal. Technol. Biomed. Life Sci.* **2012**, *898*, 111–120.
- (8) Paglia, G.; Hrafnisdottir, S.; Magnusdottir, M.; Fleming, R. M.; Thorlacius, S.; Palsson, B. O.; Thiele, I. *Anal. Bioanal. Chem.* **2012**, *402*, 1183–1198.
- (9) Spagou, K.; Wilson, I. D.; Masson, P.; Theodoridis, G.; Raikos, N.; Coen, M.; Holmes, E.; Lindon, J. C.; Plumb, R. S.; Nicholson, J. K.; Want, E. J. *Anal. Chem.* **2011**, *83*, 382–390.
- (10) Want, E. J.; Wilson, I. D.; Gika, H.; Theodoridis, G.; Plumb, R. S.; Shockcor, J.; Holmes, E.; Nicholson, J. K. *Nat. Protoc.* **2010**, *5*, 1005–1018.
- (11) Laphorn, C.; Pullen, F.; Chowdhry, B. Z. *Mass Spectrom. Rev.* **2013**, *32*, 43–71.

- (12) Harry, E. L.; Weston, D. J.; Bristow, A. W.; Wilson, I. D.; Creaser, C. S. *J. Chromatogr., B: Anal. Technol. Biomed. Life Sci.* **2008**, *871*, 357–361.
- (13) Dwivedi, P.; Schultz, A. J.; Hill, H. H. *Int. J. Mass Spectrom.* **2010**, *298*, 78–90.
- (14) Dwivedi, P.; Puzon, G.; Tam, M.; Langlais, D.; Jackson, S.; Kaplan, K.; Siems, W. F.; Schultz, A. J.; Xun, L.; Woods, A.; Hill, H. H., Jr. *J. Mass Spectrom.* **2010**, *45*, 1383–1393.
- (15) Malkar, A.; Devenport, N. A.; Martin, H. J.; Patel, P.; Turner, M. A.; Watson, P.; Maughan, R. J.; Reid, H. J.; Sharp, B. L.; Thomas, C. L. P.; Reynolds, J. C.; Creaser, C. S. *Metabolomics* **2013**, *9*, 1192–1201.
- (16) Kaplan, K.; Dwivedi, P.; Davidson, S.; Yang, Q.; Tso, P.; Siems, W.; Hill, H. H., Jr. *Anal. Chem.* **2009**, *81*, 7944–7953.
- (17) Kanu, A. B.; Dwivedi, P.; Tam, M.; Matz, L.; Hill, H. H., Jr. *J. Mass Spectrom.* **2008**, *43*, 1–22.
- (18) Castro-Perez, J.; Roddy, T. P.; Nibbering, N. M.; Shah, V.; McLaren, D. G.; Previs, S.; Attygalle, A. B.; Herath, K.; Chen, Z.; Wang, S. P.; Mitnaul, L.; Hubbard, B. K.; Vreeken, R. J.; Johns, D. G.; Hankemeier, T. *J. Am. Soc. Mass Spectrom.* **2011**, *22*, 1552–1567.
- (19) Chong, W. P.; Goh, L. T.; Reddy, S. G.; Yusufi, F. N.; Lee, D. Y.; Wong, N. S.; Heng, C. K.; Yap, M. G.; Ho, Y. S. *Rapid Commun. Mass Spectrom.* **2009**, *23*, 3763–3771.
- (20) Ridenour, W. B.; Kliman, M.; McLean, J. A.; Caprioli, R. M. *Anal. Chem.* **2010**, *82*, 1881–1889.
- (21) Kliman, M.; May, J. C.; McLean, J. A. *Biochim. Biophys. Acta* **2011**, *1811*, 935–945.
- (22) Hart, P. J.; Francese, S.; Claude, E.; Woodroffe, M. N.; Clench, M. R. *Anal. Bioanal. Chem.* **2011**, *401*, 115–125.
- (23) Shah, V.; Castro-Perez, J. M.; McLaren, D. G.; Herath, K. B.; Previs, S. F.; Roddy, T. P. *Rapid Commun. Mass Spectrom.* **2013**, *27*, 2195–2200.
- (24) Sigurdsson, V.; Hilmarsdottir, B.; Sigmundsdottir, H.; Fridriksdottir, A. J.; Ringner, M.; Villadsen, R.; Borg, A.; Agnarsson, B. A.; Petersen, O. W.; Magnusson, M. K.; Gudjonsson, T. *PLoS One* **2011**, *6*, e23833.
- (25) Giles, K. *Int. J. Ion Mobility Spectrom.* **2013**.
- (26) Bush, M. F.; Campuzano, I. D.; Robinson, C. V. *Anal. Chem.* **2012**, *84*, 7124–7130.
- (27) Williams, J. P.; Lough, J. A.; Campuzano, I.; Richardson, K.; Sadler, P. J. *Rapid Commun. Mass Spectrom.* **2009**, *23*, 3563–3569.
- (28) Fenn, L. S.; Kliman, M.; Mahsut, A.; Zhao, S. R.; McLean, J. A. *Anal. Bioanal. Chem.* **2009**, *394*, 235–244.
- (29) Bolton, E. E.; Wang, Y.; Thiessen, P. A.; Bryant, S. H. *Annu. Rep. Comput. Chem.* **2008**, *4*, 217–241.
- (30) Frisch, M. J.; Trucks, G. W.; Schlegel, H. B.; Scuseria, G. E.; Robb, M. A.; Cheeseman, J. R.; Scalmani, G.; Barone, V.; Mennucci, B.; Petersson, G. A.; Nakatsuji, H.; Caricato, M.; Li, X.; Hratchian, H. P.; Izmaylov, A. F.; Bloino, J.; Zheng, G.; Sonnenberg, J. L.; Hada, M.; Ehara, M.; Toyota, K.; Fukuda, R.; Hasegawa, J.; Ishida, M.; Nakajima, T.; Honda, Y.; Kitao, O.; Nakai, H.; Vreven, T.; Montgomery, J. A., Jr.; Peralta, J. E.; Ogliaro, F.; Bearpark, M.; Heyd, J. J.; Brothers, E.; Kudin, K. N.; Staroverov, V. N.; Kobayashi, R.; Normand, J.; Raghavachari, K.; Rendell, A.; Burant, J. C.; Iyengar, S. S.; Tomasi, J.; Cossi, M.; Millam, N. J.; Klene, M.; Knox, J. E.; Cross, J. B.; Bakken, V.; Adamo, C.; Jaramillo, J.; Gomperts, R. E.; Stratmann, O.; Yazyev, A. J.; Austin, R.; Cammi, C.; Pomelli, J. W.; Ochterski, R.; Martin, R. L.; Morokuma, K.; Zakrzewski, V. G.; Voth, G. A.; Salvador, P.; Dannenberg, J. J.; Dapprich, S.; Daniels, A. D.; Farkas, O.; Foresman, J. B.; Ortiz, J. V.; Cioslowski, J.; Fox, D. J. *Gaussian 09*; Gaussian Inc.: Wallingford, CT, 2009.
- (31) Menikarachchi, L. C.; Cawley, S.; Hill, D. W.; Hall, L. M.; Hall, L.; Lai, S.; Wilder, J.; Grant, D. F. *Anal. Chem.* **2012**, *84*, 9388–9394.
- (32) Campuzano, I.; Bush, M. F.; Robinson, C. V.; Beaumont, C.; Richardson, K.; Kim, H.; Kim, H. I. *Anal. Chem.* **2012**, *84*, 1026–1033.
- (33) Mesleh, M. F.; Hunter, J. M.; Shvartsburg, A. A.; Schatz, G. C.; Jarrold, M. F. *J. Phys. Chem.* **1996**, *100*, 16082–16086.
- (34) Shvartsburg, A. A.; Jarrold, M. F. *Chem. Phys. Lett.* **1996**, *261*, 86–91.

- (35) Wishart, D. S.; Jewison, T.; Guo, A. C.; Wilson, M.; Knox, C.; Liu, Y.; Djoumbou, Y.; Mandal, R.; Aziat, F.; Dong, E.; Bouatra, S.; Sinelnikov, I.; Arndt, D.; Xia, J.; Liu, P.; Yallou, F.; Bjornrdahl, T.; Perez-Pineiro, R.; Eisner, R.; Allen, F.; Neveu, V.; Greiner, R.; Scalbert, A. *Nucleic Acids Res.* **2013**, *41*, D801–807.
- (36) Smith, C. A.; O'Maille, G.; Want, E. J.; Qin, C.; Trauger, S. A.; Brandon, T. R.; Custodio, D. E.; Abagyan, R.; Siuzdak, G. *Ther. Drug Monit.* **2005**, *27*, 747–751.
- (37) Zhu, Z. J.; Schultz, A. W.; Wang, J.; Johnson, C. H.; Yannone, S. M.; Patti, G. J.; Siuzdak, G. *Nat. Protoc.* **2013**, *8*, 451–460.
- (38) Fu, W.; Magnusdottir, M.; Brynjolfson, S.; Palsson, B. O.; Paglia, G. *Anal. Bioanal. Chem.* **2012**, *404*, 3145–3154.
- (39) Castro-Perez, J. M.; Kamphorst, J.; DeGroot, J.; Lafeber, F.; Goshawk, J.; Yu, K.; Shockcor, J. P.; Vreeken, R. J.; Hankemeier, T. *J. Proteome Res.* **2010**, *9*, 2377–2389.
- (40) Evans, A. M.; Mitchell, M. W.; Dai, H.; DeHaven, C. D. *Metabolomics: Open Access* **2012**, *2*, 110.
- (41) Distler, U.; Kuharev, J.; Navarro, P.; Levin, Y.; Schild, H.; Tenzer, S. *Nat. Methods* **2014**, *11*, 167–170.
- (42) Geromanos, S. G.; Hughes, C.; Ciavarini, S.; Vissers, J. P. C.; Langridge, J. I. *Anal. Bioanal. Chem.* **2012**, *404*, 1127–1139.
- (43) Bond, N. J.; Shliha, P. V.; Lilley, K. S.; Gatto, L. *J. Proteome Res.* **2013**, *12*, 2340–2353.
- (44) Aigner, K.; Dampier, B.; Descovich, L.; Mikula, M.; Sultan, A.; Schreiber, M.; Mikulits, W.; Brabletz, T.; Strand, D.; Obrist, P.; Sommergruber, W.; Schweifer, N.; Wernitznig, A.; Beug, H.; Foisner, R.; Eger, A. *Oncogene* **2007**, *26*, 6979–6988.
- (45) Peinado, H.; Olmeda, D.; Cano, A. *Nat. Rev. Cancer* **2007**, *7*, 415–428.
- (46) Sumner, L. W.; Amberg, A.; Barrett, D.; Beale, M. H.; Beger, R.; Daykin, C. A.; Fan, T. W.; Fiehn, O.; Goodacre, R.; Griffin, J. L.; Hankemeier, T.; Hardy, N.; Harnly, J.; Higashi, R.; Kopka, J.; Lane, A. N.; Lindon, J. C.; Marriott, P.; Nicholls, A. W.; Reily, M. D.; Thaden, J. J.; Viant, M. R. *Metabolomics* **2007**, *3*, 211–221.
- (47) O'Brien, P. J.; Lee, M.; Spilker, M. E.; Zhang, C. C.; Yan, Z.; Nichols, T. C.; Li, W.; Johnson, C. H.; Patti, G. J.; Siuzdak, G. *Cancer Metab.* **2013**, *1*, 4.
- (48) Paglia, G.; Ifa, D. R.; Wu, C.; Corso, G.; Cooks, R. G. *Anal. Chem.* **2010**, *82*, 1744–1750.
- (49) Fasciotti, M.; Sanvido, G. B.; Santos, V. G.; Lalli, P. M.; McCullagh, M.; de Sa, G. F.; Daroda, R. J.; Peter, M. G.; Eberlin, M. N. *J. Mass Spectrom.* **2012**, *47*, 1643–1647.